Nano Research

ISSN 1998-0124 CN 11-5974/O4
https://doi.org/10.1007/s12274-023-6184-y

Review Article

Recent Advances in Small-Scale Hydrogel-Based Robots for Adaptive Biomedical Applications

Mingzhe Nie, Qilong Zhao, Xuemin Du(✉)

[1] Institute of Biomedical & Health Engineering, Shenzhen Institute of Advanced Technology (SIAT), Chinese Academy of Sciences (CAS), Shenzhen 518055, P. R. China

Nano Res., **Just Accepted Manuscript** • https://doi.org/10.1007/s12274-023-6184-y
http://www.thenanoresearch.com on Sep. 13, 2023

Just Accepted

Address correspondence to First A. Firstauthor, email1; Third C. Thirdauthor, email2

Recent Advances in Small-Scale Hydrogel-Based Robots for Adaptive Biomedical Applications

Mingzhe Nie, [1] *Qilong Zhao,* [1] *and Xuemin Du** [1]

[1]Dr. M. Nie, Dr. Q. Zhao, and Prof. Dr. X. Du

Institute of Biomedical & Health Engineering, Shenzhen Institute of Advanced Technology (SIAT), Chinese Academy of Sciences (CAS), Shenzhen 518055, P. R. China

Correspondence to E-mail: xm.du@siat.ac.cn

Abstract: Small-scale robots, ranging in size from micrometers to centimeters, have gained significant attention in the biomedical field. However, conventional small-scale robots made of rigid materials encounter challenges in adapting themselves to the soft tissues and complicated environments of human body. Compared to the rigid counterpart, small-scale hydrogel-based robots hold great promises due to their tissue-like low modulus, outstanding biocompatibility and accessible stimuli-responsive capabilities. These attributes offer small-scale hydrogel-based robots with multimodal locomotion and reinforced functions, further enhancing the adaptability in manipulation and tasks execution for various biomedical applications. In this review, we present recent advances in small-scale hydrogel-based robots. We first summarize the design principles of small-scale hydrogel-based robots including materials, fabrication techniques and manipulation strategies, then highlighting their upgraded functions and adaptive biomedical applications. Finally, we discuss existing challenges and future perspectives for small-scale hydrogel-based robots.

Keywords: small-scale robot, hydrogel, locomotion, multi-function, adaptability

1. Introduction

Small-scale robots, ranging in size from micrometers to centimeters [1, 2], that can be remotely controlled by light [3, 4], acoustic [5, 6], electric [7, 8], and magnet [9-13], have shown great promise in the field of biomedical applications [14, 15]. Due to their small size, programmable locomotion and actuation behaviors, they can perform various tasks in confined spaces within human bodies, providing significant advances in disease therapies and diagnostics [16, 17]. For example, slippery micropropellers can be magnetically controlled to penetrate through the dense vitreous humor to reach retina [18]. Moreover, small-scale robots also enable deep tissue imaging and real-time tracking *in vivo* [19]. Despite great promises in disease therapies and diagnostics, conventional small-scale robots made of rigid materials such as metals and ceramics encounter challenges in adapting to the soft tissues of human body. This issue arises because of mechanical mismatch and conflicts between the predetermined robot body and the unstructured environments in human body [20]. Developing small-scale robots with tunable material properties, low modulus (from 1 to 10^3 kPa), and the capability of accomodating different scenarios presented by different tissues is of utmost importance to reduce the risk of tissue damage and achieve reliable tasks in physiological environments [21].

In recent years, there has been a growing interest in the use of soft materials with similar mechanics to those of soft tissues, such as elastomers [22, 23], shape memory polymers [24, 25] and hydrogels [26-28], for biomedical applications. These materials offer significant advantages over rigid materials for creating small-scale robots with improved adaptability, making them highly promising for biomedical applications. In particular, hydrogels show excellent promise due to their tissue-like viscoelastic mechanics [29, 30], good biocompatibility [31, 32], and stimuli-responsive capabilities [33-37]. By incorporating functional fillers that can be actuated by environmental stimuli or external fields into hydrogel body matrix, a range of small-scale hydrogel-based robots that can move toward targeted sites have been developed, reprensenting a new trend of the filed [38-40]. The hydrogel bodies contribute to the robots' outstanding adaptability and compliance during programming and directional locomotion. Moreover, integrating stimuli-responsive capabilities via elaborately designed within hydrogel bodies allows small-scale hydrogel-based robots to achieve multiple functions such as shape reconfiguration, camouflage, and environmental interaction [41, 42]. Advances in materials have further enhanced the adaptability of small-scale robots in manipulation and performing difficult tasks within the complex dynamic environments of human bodies, bringing breakthroughs for various biomedical applications such as cell capture, target drug delivery, biopsy, minimally invasive surgery and neural stimulation (**Figure 1**).

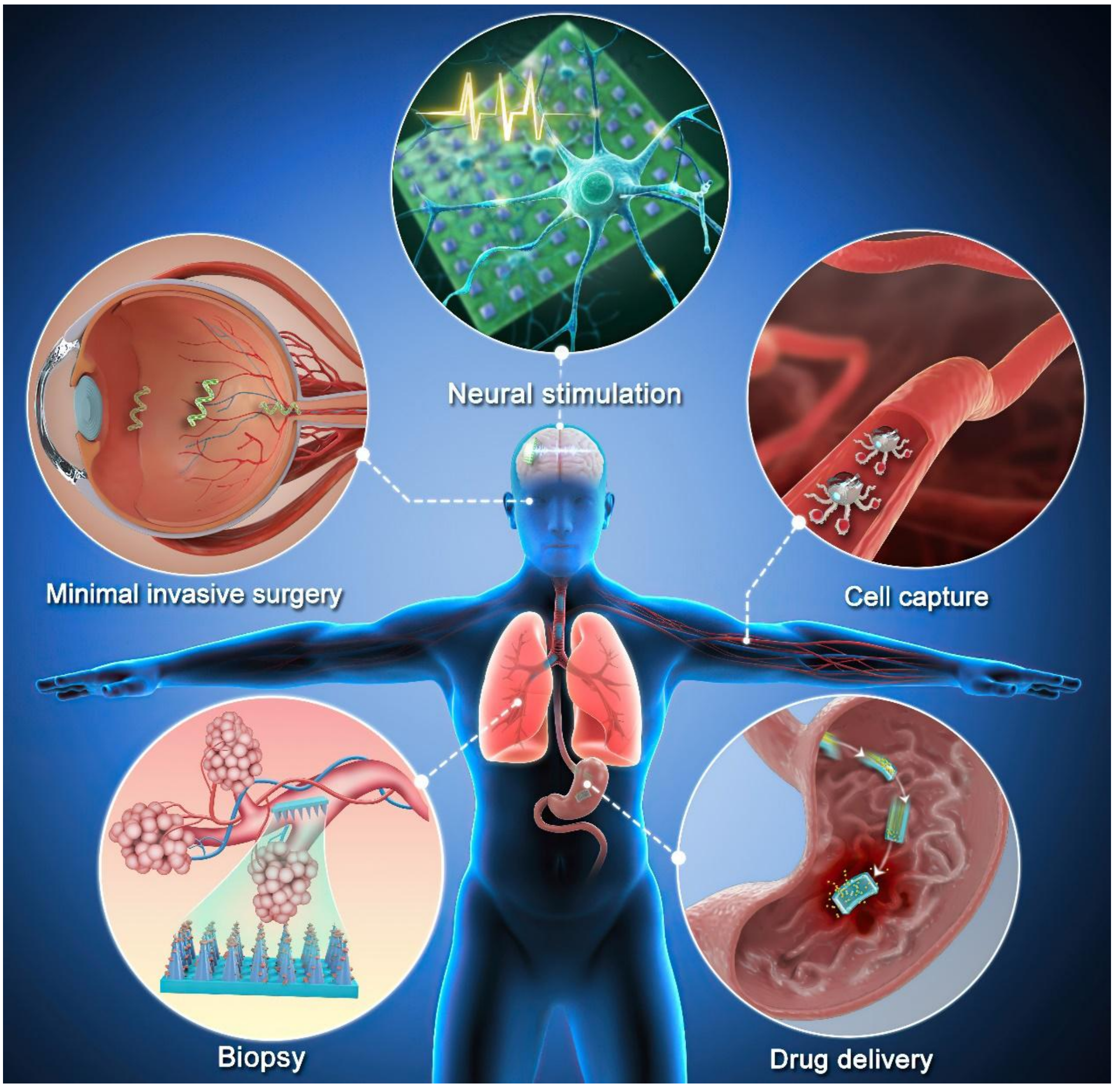

Figure 1. Illustration of small-scale hydrogel-based robots in various biomedical applications including cell capture, target drug delivery, biopsy, minimally invasive surgery and neural stimulation.

Despite numerous reviews on small-scale robots, these progresses usually focused on actuating materials [26], or driving mechanisms [39, 40]. However, there still lacks a comprehensive review, which focuses on the adaptability of small-scale robots for biomedical applications. In this review, we will summarize the recent advances in small-scale hydrogel-based robots for adaptive biomedical applications. First, we will provide an overview of the materials and techniques for fabricating small-scale hydrogel-based robots, as well as their manipulation approaches. Next, we will highlight the design of small-scale hydrogel-based robots with upgraded functions, especially their potential for enhancing adaptabilities. Furthermore, we will discuss their biomedical applications including target drug/cell delivery, minimally invasive surgery, biopsy and neural stimulation, where their upgraded functions result in improved adaptability. Finally, we will address current challenges and prospects related to the future developments of small-scale hydrogel-based robots wiht the aim of obtaining superior adaptability and intelligence to accomodate complex dynamic pathophysiology for advanced diagnostics and disease therapies.

2 Design principles for small-scale hydrogel-based robots

2.1 Materials

In order to achieve optimal adaptability in human bodies, not only the small-scale hydrogel-based robots shall possess suitable shapes or sizes, but also the materials for constructing small-scale hydrogel-based robots shall possess appropriate mechanical properties, biocompatibility or biodegradability, and function integration capabilities (**Table 1**). Specifically, the materials should not be too rigid or brittle, nor should they be too soft to be effectively controlled in high-viscosity environments such as bodily fluids. Additionally, they must exhibit minimal toxicity to cells and organs, and ideally be safely cleared or degraded by the human body. Incorporating multiple functions, such as shape reconfiguration and camouflage, would further enhance environmental adaptability and the capability of task execution.

A wide range of natural and synthetic materials, both responsive and non-responsive, have been explored for creating small-scale hydrogel-based robots. Natural materials like chitosan [43], calcium alginate [44, 45], gelatin [46, 47], starch [48], gelatin methacrylate (GelMA) [49], DNA [50] and sugar [51] have been studied for their excellent biocompatibility and mild crosslinking conditions for forming hydrogel bodies. For example, the super-softness and super-elasticity of the magnetic

DNA hydrogel (elastic modulus was lower than 1 Pa) showed navigational locomotion in confined and unstructured space under a magnetic field [50]. Meanwhile, synthetic materials such as poly (acryl amide) (PAAm) [52, 53], poly (vinyl alcohol) (PVA) [54, 55], poly (ethylene glycol) diacrylate (PEGDA) [56, 57] and poly (2-hydroxyethyl methacrylate) (PHEMA) [58] have been investigated due to their ability to enhance the mobility of small-scale hydrogel-based robots. Compared to natural hydrogel-based robots, synthetic hydrogels offer a broader range of options for tailoring the mechanical properties of the resulting small-scale robots. Synthetic hydrogels such as PVA can have a tunable modulus (with a range from 24 ± 2 to 2500 ± 140 kPa), making them more adaptable. Stimuli-responsive synthetic hydrogels like poly (N-isopropylacrylamide) (PNIPAM) [57, 59, 60] and poly (acryl acid) (PAA) [61] have been also used for creating small-scale hydrogel-based robots with interactive capabilities. These hydrogels can respond to external stimuli, such as temperature or pH changes, resulting in impressive functions like controllable attachment and detachment to biological tissues [62]. However, concerns about the biocompatibility of synthetic hydrogels cannot be ignored. To address that, natural hydrogels with programmable stimuli-responsive behaviors have been developed via elaborate structural and molecular design [63-65]. For example, shape-morphing chitosan hydrogel film was obtained by combining gradient cross-linking density and geometry effect [63]. Combining the softness, superior biocompatibility, and programmable stimuli-responsive behaviors of hydrogels, it will be envisioned to create next-generation small-scale hydrogel-based robots with better adaptability.

Table 1. Materials, shape (size), fabrication techniques, manipulation strategies, biocompatibility and biodegradability of representative small-scale hydrogel-based robots.

Materials		Shape (Size)	Fabrication techniques	Manipulation strategies	Biocompatibility	Biodegradability	Ref.
Natural materials	Chitosan	Helical (Microscale)	3D printing	Magnetic actuation	Cell viability >90%	Enzymatic degradation	[37]
	Calcium alginate	Star shape (Microscale)	Soft lithography	Magnetic actuation	Cell viability >85%	Degradable	[45]
	Gelatin	Sphere (Microscale)	Emulsion method	Magnetic actuation	80% cell viability in 4 weeks	Degradable	[47]
	Starch	Film (Centiscale)	Soft lithography	Light actuation	Low cytotoxic effects	Degradation in soil	[48]
	GelMA	Helical (Microscale)	3D printing	Magnetic actuation	Cell viability >90%	Degrade with glutathione	[49]
	DNA	Circular	Soft lithography	Magnetic actuation	Cell viability 92.15%	Not provided	[50]

	Sugar	Helical (Microscale)	3D printing	Magnetic actuation	Low cytotoxic effects	Degradation in water	[51]
Synthetic materials	PAAm	Rod-shape (millimeter-scale)	Photolithography	Magnetic actuation	Not provided	Not provided	[53]
	PVA	Sheet (Microscale)	Soft lithography	Light actuation	Not provided	Not provided	[55]
	PNIPAM/ PEGDA	Helical (Microscale)	Photolithography	Magnetic actuation	Sustained cell growth	Not provided	[57]
	PHEMA	Gripper (Microscale)	Photolithography	Magnetic actuation	Cell viability >99.57%	Not provided	[58]
	PAA	Fish or crab (Microscale)	Photolithography	Magnetic actuation	Cell viability >96%	Not provided	[61]

2.2 Fabrication techniques

To perform specific diagnostic and therapeutic tasks in small cavities within the human bodies, it is necessary for small-scale hydrogel-based robots to possess both small sizes (ranging from micrometers to centimeters) and specially designed structures. Achieving these minimal yet intricate structures requires high-precision manufacturing techniques such as advanced micro-nano machining approaches. These techniques can be broadly classified into two strategies: top-down and bottom-up approaches (**Table 1**).

Photolithography and soft lithography are common top-down manufacturing methods that are highly effective for producing small-scale hydrogel-based robots with exceptional machining precision, versatility and scalable production. These methods afford a broad range in size spaning from hundreds of micrometers to dozens of centimeters and a multitude of pre-determined or designed structures that can be tailored to meet specific requirements [66]. Usually, photolithography employs a photomask with micro or nanoscale resolution to create elaborate structures [67], while soft lithography employs a wide range of soft replica mold, such as in the form of a polydimethylsiloxane (PDMS) template or polyurethanes (PU) or polyimides, to determine the body structures of the robots [55]. Through soft lithography, a bilayer hydrogel microrobot (one gelatin/PVA/PLGA/DOX layer and one PEGDA/MNPs layer) with sheet-type geometries and microscale dimensions has been prepared (**Figure 2a**) [55]. The small size and sheet-type body structures of these robots make it easy to inject into lesion sites by rolling the sheet-type bodies.

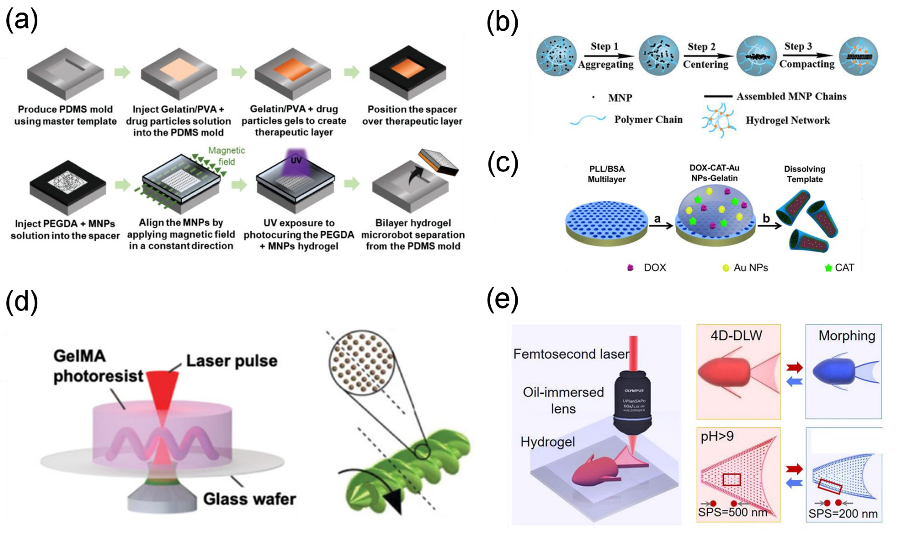

Figure 2. (a) Fabrication of bilayer sheet-type hydrogel microrobot with a PDMS soft template and photocuring. Reproduced with permission from ref. [55]. Copyright John Wiley and Sons., 2020. (b) Fabrication of micro-spheric hydrogel robot by assembling magnetic particles into the chain-like structures with hydrogel under the external static magnetic field. Reproduced with permission from ref. [68]. Copyright John Wiley and Sons., 2020. (c) Fabrication of gelatin hydrogel-based rocket-shaped microrobot. Reproduced with permission from ref. [69]. Copyright American Chemical Society, 2015. (d) 3D printing of GelMA helical magnetic robot based on TPP. Reproduced with permission from ref. [70]. Copyright John Wiley and Sons., 2020. (e) 4D printing of crab and fish with encoded point density in various body parts based on Fs-DLW. Reproduced with permission from ref. [61]. Copyright American Chemical Society, 2021.

The fabrication of small-scale hydrogel-based robots primarily utilizes bottom-up approaches such as emulsion polymerization and self-assembly. These strategies offer a high efficiency in mass production of nano- or submicro-scale hydrogel-based robots. Specifically, through emulsion polymerization, spherical magnetic microrobots with uniform sizes ranging from 45 to 55 μm could be formed by using an emulsion containing PEI, PEGDE, and magnetic nanoparticles (**Figure 2b**) [68]. Their micro-spherical structures reduced the friction and hence facilitated the locomotion of the magnetic microrobots in fluidic media. Template-assisted layer-by-layer (LbL) assembly offers the possibility of forming small-scale hydrogel-based robots with heterogeneous compositions and ordered structures. Through LbL assembly, a temperature-responsive rocket-shaped hydrogel-based robot could be formed[55], by firstly depositing poly-L-lysine/bovine serum albumin

(PLL/BSA) multilayers onto a porous polycarbonate (PC) membrane, then coated by a gelatin hydrogel with supplemented catalase (CAT), gold nanoparticles (AuNPs), and doxorubicin (DOX), and finally released from the PC membrane (**Figure 2c**) [69]. These rocket-shaped robots not only allowed for controllable loading capacity, but also could be navigated by both biocatalytic bubble propulsion of CAT and magnetic propulsion from electro-magnetic conversion from AuNPs.

To create small-scale hydrogel-based robots with both fine machining structure and sophisticated geometries, 3D printing techniques have been utilized [71]. For example, 3D printing based on two-photon polymerization (TPP) [72, 73] enables nanoscale precise manufacturing of 3D helical structures of GelMA hydrogel robot with well-defined properties and functions (**Figure 2d**). Additionally, 4D printing has enabled dynamic tailoring of sophisticated geometries and properties of hydrogel-based robots [74, 75]. For example, pH-responsive hydrogels made of PAA and fabricated by femtosecond direct laser writing (Fs-DLW) with nanoscale printing precision through 4D printing, could be morphed into various shapes, such as fish and crab, with encoded point density within their body parts (**Figure 2e**) [61]. The encoded point density determined the shape-morphing process for environmental adaption. 4D printing of small-scale hydrogel-based robots that can respond to external stimuli and change shapes would greatly enhance their functionalities.

2.3 Manipulation strategies

Programming/directional locomotion is crucial for small-scale hydrogel-based robots to move to specific sites in human body before performing their intended tasks [76]. To manipulate the programming/directional locomotion, it is essential to generate adequate asymmetric driving forces that can overcome the high viscous resistance and shear stress present in body tissues. Such tissues typically contain high-viscosity and flowing fluids, in addition to the non-negligible effects of Brownian motion that come into play down to micron scale. Even though the design of asymmetric shapes can lower resistance in a certain direction [77], the key to achieving programming/directional locomotion would still be the generation sufficient force to initiate the actuation. Generally, it would achieved by incorporating functional segments within the hydrogel bodies of the robots that can be actuated by either the robot's environment or external fields [78] **(Table 1)**.

In order to realize the environmentally controlled locomotion of small-scale hydrogel-based robots, it is necessary to convert chemical energy from the surroundings into kinetic energy [79]. It is usually achieved through the asymmetrical design of the robot. For example, a small-scale robot made from PNIPAM hydrogel with asymmetric preloading of platinum (Pt) has been designed and developed (**Figure 3a**) [80]. It could be propelled in the medium of H_2O_2 as the preloaded Pt catalyzes the decomposition of H_2O_2 to generate bubbles to promote the locomotion of the robot. The environmentally controlled locomotion could also be realized in physiologically mimicking environments. For instance, through the inclusion of biodegradable Zn or Mg with the PNIPAM hydrogel bodies, small-scale robots that can be self-propelled in the acidic environments of the stomach have been established. Their locomotion is actuated by the hydrogen bubbles generated by the reactions between the inclusive Zn /Mg and H^+ in the environments [81]. In addition, some environmentally controlled small-scale hydrogel robots can even be manipulated through enzyme-catalyzed reactions that harness various biomolecules such as glucose and urea as "fuels" [82], showing better promise in biomedicine. However, such locomotion has inherent limitations in environmental adaptability and manipulating accuracy, which may restrict the versatility scopes of the environmentally controlled small-scale hydrogel robots for biomedical applications.

Precise and remotely controlled locomotion of small-scale hydrogel-based robots has garnered significant attention. Ultrasound is utilized as an external energy source to maneuver the robots. Ultrasound waves have the ability to penetrate solid, liquid, and air media, making them highly suitable for biomedical applications as they do not cause harm to human bodies [83]. By inducing ultrasound-triggered components, a microcannon robot loaded with a gelatin-based hydrogel matrix embedded with perfluorocarbon emulsion and nanobullet was prepared. The ultrasound-triggered vaporization of the perfluorocarbon emulsion led to a rapid ejection of the nanobullet, achieving deep penetration (**Figure 3b**) [83]. Light is also an alternative approach for achieving untethered manipulation of small-scale hydrogel-based robots with high versatility and portability. Photoactive materials such as photocatalytic materials, photochromic materials, and photothermal materials are introduced as building blocks [84, 85]. For instance, a small-scale hydrogel-based robot was fabricated using polyacrylamide (PAM) hydrogel containing Fe_3O_4/Cu hybrid nanorods, combined with the top layer of polyimide (PI) and the bottom layer of polydimethylsiloxane (PDMS). The plasmonic layer containing the Fe_3O_4/Cu hybrid nanorods enables the conversion of light into heat, generating steam bubbles. This robot is fueled by water and remotely powered by light, displaying self-adaptable functions and working modes upon environmental changes (**Figure 3c**) [52]. Additionally, incorporating magnetic components such as ferromagnetic, ferrimagnetic, and superparamagnetic materials (e.g., Co, Ni, NdFeB, and Fe_3O_4) into the hydrogel matrix or forming magnetic coatings using these magnetic components could result in magnetic propulsion of small-scale hydrogel-based robots. The manipulation of magnetic-controlled small-scale hydrogel-based robots can be achieved by either directing the rotation of the magnetic moments of embedded magnetic components in a gradient magnetic field or in a time-varying magnetic field (rotating or oscillating magnetic fields) [78], [86, 87]. For example, a microswimmer composed of a thermoresponsive hydrogel embedded with magnetic particles (MNPs) was fabricated, the in-plane particle alignment of microswimmer was constant while the out-of-plane particle alignment varied. By changing the out-of-plane alignment of MNPs, the microswimmer could either rotate or directional move (**Figure 3d**) [57]. As magnetic fields can also permeate through tissues without causing any harm in a wide range of frequencies and magnitudes [12, 88-90], magnetic-actuated small-scale robots are ideally suited for biomedical applications, particularly in human bodies.

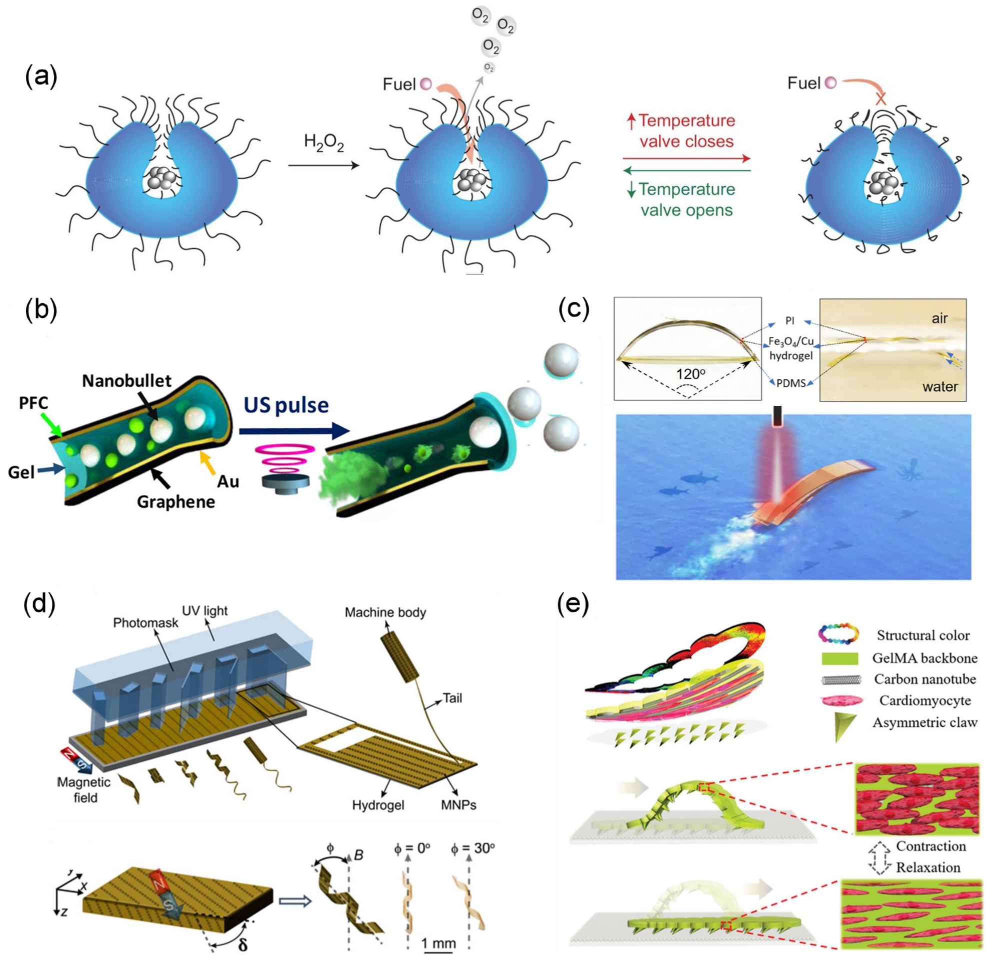

Figure 3. (a) Scheme of PNIPAM hydrogel robot preloaded with Pt that catalyzes the decomposition of H_2O_2 to generate bubbles and propel the robot. Reproduced with permission from ref. [80]. Copyright Springer Nature, 2017. (b) Scheme of ultrasound-triggered vaporization of perfluorocarbon emulsion and ejection of nanobullet inside the gelatin-based hydrogel robot. Reproduced with permission from ref. [83]. Copyright American Chemical Society, 2016. (c) The structure of trilayered hydrogel robot (top) and scheme of the hydrogel robot swimming at the air-water interface (bottom). Reproduced with permission from ref. [52]. American Association for the Advancement of Science, 2021. (d) Photolithography fabrication of hydrogel microswimmer (top) and the out-of-plane alignment ($\delta \neq 0$) of MNPs lead to the rotation of microswimmer (bottom). Reproduced with permission from ref. [57]. American Association for the Advancement of Science, 2019. (e) The crawling process of the hybrid GelMA hydrogel robot driven by contraction of cardiomyocytes. Reproduced with permission from ref. [91]. Copyright John Wiley and Sons., 2019.

In addition to environment-triggered and field-controlled manipulation, small-scale hydrogel-based robots can also be actuated by living cells. These robots are typically hybrids of hydrogels and specific living cells [92] such as microorganisms (including bacteria and sperm), and mammalian cells. The living cells act as engines to propel the biohybrid small-scale robots. For instance, a biohybrid small-scale robot made of GelMA composite hydrogel and cardiomyocytes was created. By utilizing the contraction of cardiomyocytes, the hybrid small-scale robot achieved directional crawling locomotion (**Figure 3e**) [91]. Owing to their biohybrid compositions, these robots showed significantly improved biocompatibility and biosafety. These biohybrid robots that mimic the organisms in nature would greatly enhance their adaptability within the human body.

3. Adaptive small-scale hydrogel-based robots

The intrinsic properties of hydrogels such as tissue-like viscoelasticity and hence desirable mechanical compliance to biological tissues have brought small-scale hydrogel-based robots with excellent adaptability in mechanics for biomedical applications [21]. In addition, the ease of functionalization for hydrogels could even result in adaptive small-scale hydrogel-based robots, possessing upgraded adaptabilities that accommodate dynamic and complex environments in human bodies. By selecting hydrogels with non-responsive or stimuli-responsive properties, various strategies have been developed to enhance their effectiveness in locomotion and performing specific diagnostic and therapeutic tasks.

3.1 Mono-functional small-scale hydrogel robots

For adapting to different manipulation environments, small-scale robots made of non-responsive hydrogels, which undergo no volumetric changes or phase transitions, are often designed to possess different locomotion modes. For example, small-scale hydrogel robots can swim in the fluid environment of blood vessels, crawl in the coarse land environment of stomach, and jump in the gas-filled environment of lungs. They also achieve multimode motions under magnetic actuation by programming different magnetic domains. Since physiological environments usually contain a viscous fluidic medium, swimming is an efficient mode for the locomotion of these small-scale robots based on hydrogels. To achieve high-efficiency swimming within high-viscosity liquid mediums, a rod-shaped robot composed of polyacrylamide (PAAm) hydrogel and hard magnetic NdFeB@SiO_2 particles was constructed (as shown in **Figure 4a**) [53]. The NdFeB@SiO_2 particles were incorporated into the PAAm hydrogel section, while the non-magnetic PAAm hydrogel formed the non-magnetic sections of the robots. By using a time-varying magnetic field, the robot was able to undergo geometrical transformations from slender to arc shape, thus achieving high motility (0.71 body length per motion cycle) and upstream locomotion in a flowing fluid. These locomotion modes greatly enhance the adaptability of small-scale hydrogel-based robots to high-viscosity fluidic environments.

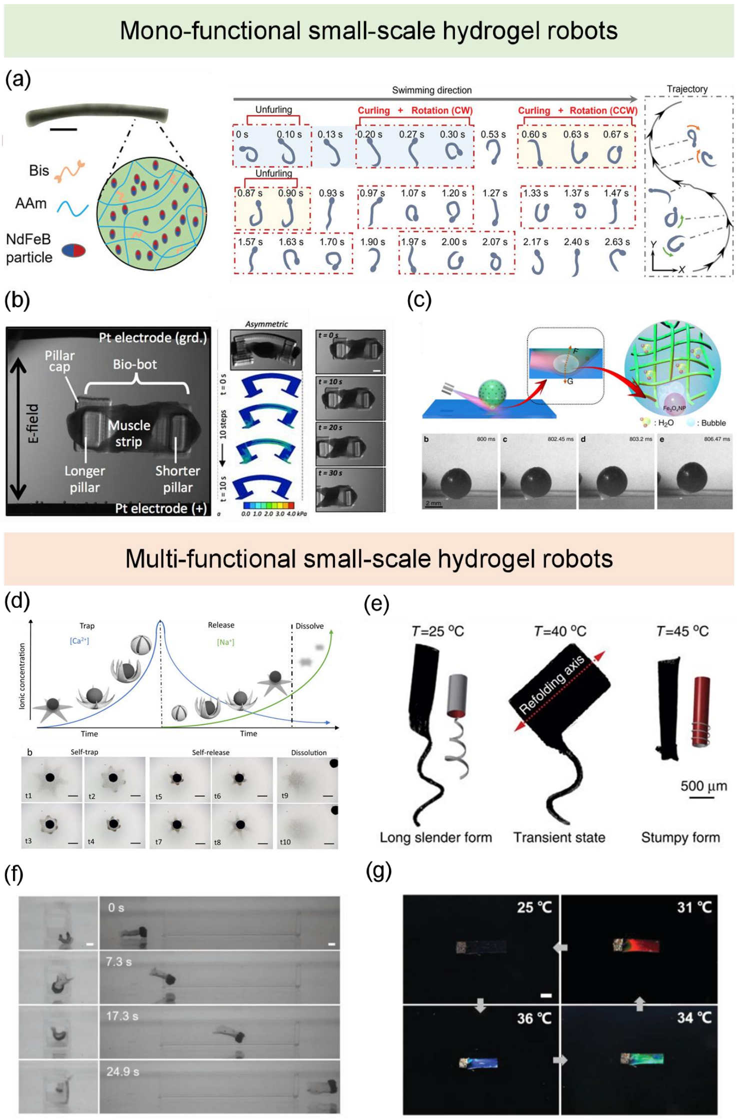

Figure 4. (a) Structure of PAAM composite hydrogel robot and the swimming behavior under magnetic field. Reproduced with permission from ref. [53]. Copyright John Wiley and Sons., 2022. (b) Crawling locomotion of biohybrid PEGDA hydrogel robot. Scale bar: 1 mm. Reproduced with permission from ref. [93]. Copyright National Academy of Sciences, 2014. (c) Schematic illustration of the jumping of the hydrogel robot caused by water vaporization due to the photothermal effect of embedded magnetic particles under light irradiation.

Reproduced with permission from ref. [94]. Copyright Springer Nature, 2020. (d) Self-trapping and self-releasing of a magnetic microsphere upon application of a $CaCl_2$ solution and a sodium citrate solution, respectively. Scale bar: 500 μm. Reproduced with permission from ref. [95]. Copyright Springer Nature, 2021. (e) A reconfigurable compound soft micromachine switching shapes between a long slender form and a compact stumpy form. Reproduced with permission from ref. [96]. Copyright Springer Nature, 2016. (f) (g) The adaptive functions of reconfiguration (The squeezed robot crawls through the small size tube in 24 s) (left), and color-shifting of the millimeter-scale PNIPAM hydrogel robot (right). Scale bar: 1 mm. Reproduced with permission from ref. [97]. Copyright John Wiley and Sons., 2020.

In specific occasions such as narrow channels and small cavities exist within the human body, crawling can be an effective locomotion mode for small-scale hydrogel-based robots. For instance, researchers have developed a millimeter-scale biological robot comprising poly (ethylene glycol) diacrylate (PEGDA) hydrogel, stiff pillars, and 3D muscle strips assembled by the skeletal muscle myoblasts (**Figure 4b**) [93]. Under electrical stimulation, the 3D muscle strips enabled the contraction of an asymmetric compliant hydrogel robot and generated enough force to power the hydrogel robot, enabling inchworm-like directional crawling locomotion with a high velocity.

To overcome obstacles during the locomotion of small-scale hydrogel-based robots in human bodies, jumping robots have also been developed. For example, a composite robot made of iron oxide nanoparticle (Fe_3O_4) and poly (sodium acrylate) (PAANa) hydrogel was fabricated (**Figure 4c**) [94]. Upon light irradiation, gas bubbles were generated inside the hydrogel robot due to the vaporization of water caused by the photothermal effect of the embedded magnetic particles. The expanded hydrogel robot hit the substrate, and the counter interaction in turn led to the jumping of the hydrogel robot (jumping height of 15 cm). The high jumping height imparted the small-scale hydrogel-based robots to negotiate high obstacles of several centimeters.

To further enhance the environmental adaptability, small-scale hydrogel-based robots integrating multimodal locomotion modes were prepared. Specifically, a magnetic micro-sized robot made of magnetic spherical Janus microparticles (silica microparticles half coated with permalloy layer, Au layer, and polyethylene glycol (PEG) layer) linked by gelatin hydrogel was fabricated [46]. By controlling the orientation of the easy axis of magnetization of each microactuator under a magnetic field, 1D and 2D chains of magnetic micro-robots with different Janus particles can dynamically shape deformation and locomotion under varying magnetic fields, 2D-legged microrobots were assembled to achieve different walking gaits (*e.g.*, rolling, wobbling, and walking) under an oscillating magnetic field. These multimodal locomotion modes allowed small-scale robots to adapt to different scenarios.

3.2 Multi-functional small-scale hydrogel robots

Small-scale robots made of hydrogels are capable of moving efficiently in various environments using different modes of locomotion. However, they still encounter difficulties accomplishing specific tasks in complex surroundings. To improve their adaptability to perform particular tasks, adaptive small-scale robots composed of stimuli-responsive hydrogels incorporating multiple functionalities, such as shape reconfiguration, camouflage, and environmental interaction capabilities, have been developed [98, 99].

The introduction of shape reconfiguration is important to enhance the adaptability of small-scale hydrogel-based robots. Shape reconfiguration such as tunable stiffness and shape-morphing behaviors have been employed to formulate small-scale hydrogel-based robots. For the tunable stiffness of small-scale hydrogel-based robots, a non-Newtonian fluid-based magnetic slime was constructed by incorporating magnetic particles (NdFeB) and borax into a polyvinyl alcohol (PVA) hydrogel [100]. The magnetic slime showed tunable stiffness by harnessing the magnetorheological effect due to the magnetic interaction between adjacent particles upon magnetization under a magnetic field. Benefiting from the deformation capabilities due to the softness, magnetic slime could not only cross narrow channels of 1.5 mm under an external magnetic field but also adapt to complex boundaries, showing both active and passive deformation behaviors.

In some scenarios, the robot is required to flexibly change shapes so that it can adapt to such environments. It hence set a higher degree of freedom of locomotion for small-scale robots. Shape deformation can change its shape under various stimuli, which is an effective way to improve the freedom of motion. For example, a shape-morphing alginate hydrogel microrobot was fabricated **(Figure 4d)** [95], and the heterogeneous electric field generate an inhomogeneous alginate hydrogel network density by controlling the concentration of Ca^{2+} in the electrodeposition process. By taking advantage of reliable shape morphing and remote magnetic control in a physiological environment, magnetic propulsion and switchable shapes can be used as a widely adaptive platform. Under ionically stimulated shrinkage or swelling of the alginate hydrogel, heterogeneous deformation of the network leads to environmentally adaptive releasing or folding motion. Moreover, the combination of shape deformation and time-varying magnetic field, it can further enhance the motion freedom. A microrobot consisting of a tubular head and monolayer helical tail structure was constructed **(Figure 4e)** [96], where a non-swelling supporting hydrogel layer of poly (ethylene glycol) diacrylate (PEGDA) and magnetic particles selectively patterned on a monolayer of swelling thermo-responsive composite hydrogel layer (PNIPAM/PAAm/PEDGA and magnetic particles). The introduction of magnetic particles endows the remote magnetic manipulation and enhanced near-infrared (NIR) responsiveness of the micro-robot. Selectively aligning the magnetic particles in different parts endow a multitude of magnetic axis, leading to tailored shape and magnetic anisotropy. The microrobot rotates along the long axis and performs corkscrew motion under a rotating magnetic field. Moreover, the microrobot can reversibly transform from a long slender to a stumpy form when exposed to NIR heating, giving rise to different forward speeds. NIR irradiation provided additional shape transformations to control propulsion under a magnetic field, affording programmable motility and morphology. Shape reconfiguration offers more possibilities for changing motion modes, which greatly increases the adaptability of small-scale hydrogel-based robots.

To further enhance the adaptabilities to complex conditions, camouflage and environmental interactions are also introduced into small-scale hydrogel-based robots. Our group fabricated a millimeter-scale robot with a head and tail structure design, where neodymium-iron-boron (NdFeB) magnetic microparticles embedded in the head of hydrogel (poly(N(isopropyl acrylamide), PNIPAM) **(Figure 4f and 4g)** [97]. The millirobots can achieve multimodal locomotion and excellent capability of helical propulsion. Owning to the temperature-responsive PNIPAM hydrogel embedded with gold nanorods (AuNRs), the millirobots undergo a ~35% of volume shrinking when crossing the narrow tube under near-infrared (NIR, 808 nm) irradiation. Moreover, visible color-shifting under varied temperatures also provided an optical camouflage in water, leading to enhanced interaction with changing environment.

4. Biomedical applications of small-scale hydrogel-based robots

4.1. Drug/cell delivery

Drug and cell delivery are crucial in the treatment of diseases as they allow for precise and controlled doses to be administered within the human body [101, 102]. Small-scale hydrogel-based robots have the abilities of loading and delivering, various drug molecules or cells to access targeted sites that may be difficult for other interventional devices. As drug and cell delivery systems, the design of these robots should consider the release profile and the preservation of the activity and viability of the cargo molecules and cells[103]. For sustainable drug delivery, small-scale hydrogel-based robots have been developed [58]. For example, a microswimmer comprised of gelatin methacryloyl (GelMA) and biofunctionalized superparamagnetic iron oxide nanoparticles were constructed (**Figure 5a**) [104]. The microswimmer was actuated by a rotating magnetic field that exerted a magnetic torque along the microswimmer's long axis. Along with the rapid degradation of the microswimmer in 118 h to solubilized nontoxic products, pathological concentrations of MMP-2, anti-ErbB 2 antibody-tagged magnetic nanoparticles were released from the fully degraded microswimmers for targeted labeling of SKBR3 breast cancer cells. By changing the composition of degradable small-scale robots, it is possible to control the release rates of the cargo molecules. For example, magneto-responsive microneedle robots consisting of the magnetic substrate (PEGDA doped with magnetizable NdFeB particles), the separable connection (bovine serum albumin (BSA) and a low concentration of GelMA), and the tips loaded with insulin (GelMA) was constructed (**Figure 5b**) [105]. These microneedle robots were encapsulated inside the commercial enteric capsule. With the programmed magnetization of the magnetic substrate, the tips of the microneedle robots can be oriented to the small intestinal wall, overcome the barriers, and be inserted into the tissue. After the separable connection degraded, the residue tips inside the tissue and degraded gradually to deliver the insulin for the treatment of diabetes. However, the drug-releasing time depending on degradation is not controllable in complex environments.

To achieve controlled drug release, an external field-assisted drug release system was introduced into small-scale hydrogel-based robots. For example, a helical poly (ethylene glycol) diacrylate (PEGDA)-pentaerythritol triacrylate (PETA) hydrogel microrobot that encapsulates Fe_3O_4 magnetic particles and the anticancer drug 5-fluorouracil (5-FU) was designed (**Figure 5c**) [6]. The microrobot followed a corkscrew locomotion to a targeted area under a rotating magnetic field in a fluidic environment, upon reaching the desired site, an ultrasonic beam was applied to trigger shear-force mediated drug release. Moreover, drug release from the microrobot can be controlled via three modes of ultrasound exposure: natural, burst, and constant.

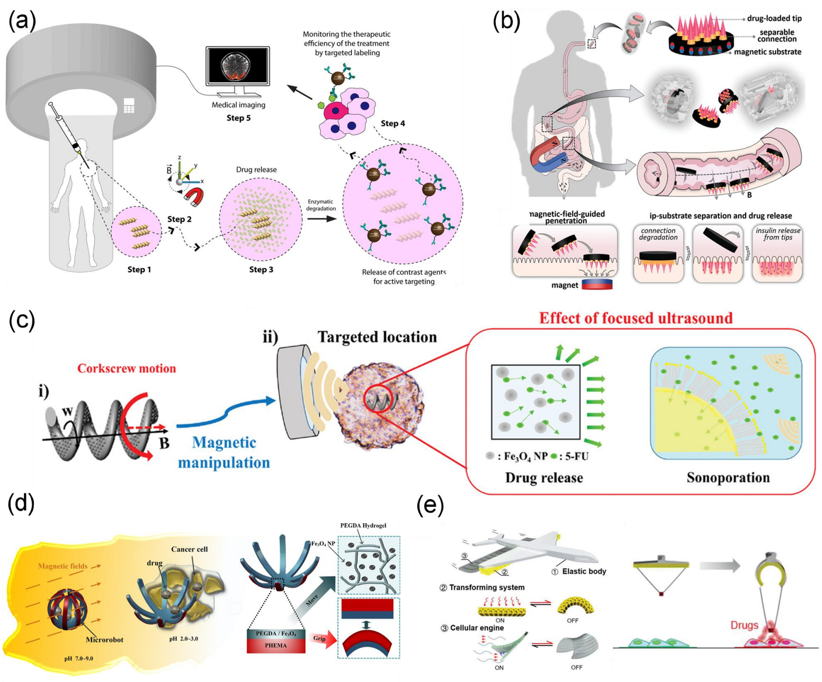

Figure 5. (a) A GelMA hydrogel microswimmer biodegrades for sustainable drug delivery [104]. Reproduced with permission from ref. [104]. Copyright American Chemical Society, 2019. (b) Schematic illustration of drug delivery process of the magnetic microneedle hydrogel robots [105]. Reproduced with permission from ref. [98].

Copyright John Wiley and Sons., 2021. (c) Schematic illustration of ultrasound-mediated drug delivery [6]. Reproduced with permission from ref. [6]. Copyright IOP Publishing, 2021. (d) Schematic illustration of the magnetic microrobot trap and release drug beads by its folding and unfolding motions at different pH values [106]. (e) Delivery of drug from the biohybrid plane-shaped hydrogel robot [107]. Reproduced with permission from ref. [107]. Copyright John Wiley and Sons., 2014.

In addition to external field-assisted drug delivery, shape deformations were also used to achieve controlled drug delivery of small-scale hydrogel-based robots. The combination of locomotion and shape deformations contribute to achieving spatiotemporally controlled drug or cell release. For example, a bilayer soft microrobot was constructed, where the PHEMA layer as a pH-responsive gel for trapping and unfolding motion of the soft microrobot in pH-varying solution (**Figure 5d**) [106], and the PEGDA-with-Fe_3O_4 layer is employed for the locomotion of the soft microrobot under magnetic field. The soft microrobot showed a moving velocity of about 600 μm s^{-1} through the generated magnetic field of the EMA system. The soft microrobot is trapped with anti-cancer drug microbeads (PCL-DTX) at about pH 9.58 and unfolds the drugs at about pH 2.6. Besides the pH-triggered delivery, drug delivery in a remotely controlled manner was also developed. Microrobots encapsulating magnetic alginate microbeads loaded with model drugs into a folded near-infrared light (NIR) responsive PNIAPM bilayer hydrogel was designed (**Figure 5e**) [107]. The closed microrobots enabling remote actuation follow the preplanned trajectory in a physiological environment under a rotational magnetic field, the closed microrobots unfold and release the drugs upon NIR irradiation. A biohybrid-controlled drug delivery system was also reported, a plane-shaped swimming robot consisting of an elastic body, transforming system, and actuation system was constructed, the soft robot is actuated by a cellular engine, and it can transform from a spread to a retracted form in respond to near-infrared light, leading to switching on or off the cellular engine. The soft robot was loaded with chemotherapeutic agents hooked on the wings of the robot to achieve drug delivery. Upon arrival at the desired site, the wings were retracted under NIR irradiation, and the hooked drug was released to bomb the cancer cells due to the lowered wings with excellent controllability and responsiveness.

4.2. Minimal invasive surgeries

Small-scale hydrogel-based robots are able to reach the desired sites under external stimuli, they can realize precise medical intervention or disease treatment in a minimally invasive manner. With the assistance of advanced imaging equipment, small-scale hydrogel-based robots can be controlled in a closed-loop manner, further improving the precision and controllability of minimally invasive surgery.

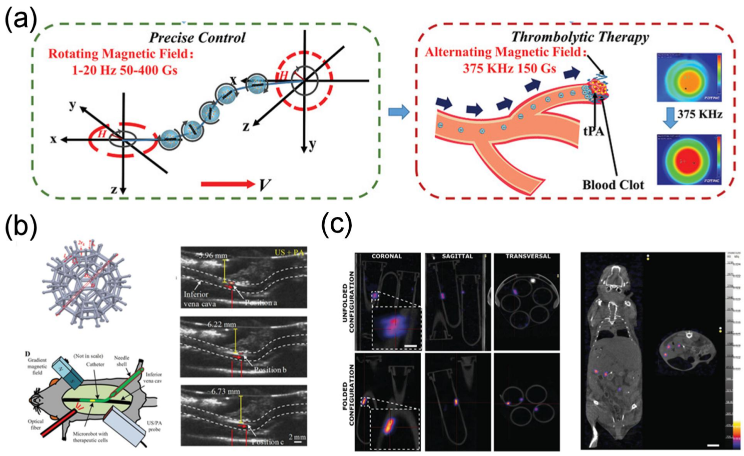

Figure 6. (a) Schematic illustration of the micro-spheric hydrogel robot for targeted thrombolysis. Reproduced with permission from ref. [68]. Copyright John Wiley and Sons., 2020. (b) Image-guided navigation of PEGDA based hydrogel microrobot with burr-like spherical structure. Reproduced with permission from ref. [108]. Copyright John Wiley and Sons., 2020. (c) Schematic illustration of real-time PA imaging of hydrogel robot and shape transformations. Scale bar: 10 mm. Reproduced with permission from ref. [109]. Copyright John Wiley and Sons., 2019.

Minimally invasive medical intervention or disease treatment of small-scale hydrogel-based robots is achieved using various strategies. For example, a swarm of small-scale hydrogel-based robots was also designed for disease treatment (**Figure 6a**) [68]. A swarm of magnetic spherical robots with tissue plasminogen activator (tPA) was first navigated to the blood clot site in artificial vasculature by a rotating magnetic field. After the swarm of magnetic spherical robots gathered at the blood clot in a glass artificial vasculature, magnetic hyperthermia treatment was carried out by an alternating magnetic field and tPA was released for thrombolysis.

To achieve closed-loop controlled targeted therapy, small-scale hydrogel-based robots need to be precisely located and monitored, and even send feedback [103]. Therefore, imaging-guided surgeries of small-scale hydrogel-based robots are also developed. For instance, PEGDA based hydrogel microrobot with a burr-like porous spherical structure for *in vivo* real-time imaging was obtained (**Figure 6b**) [108]. With a photoacoustic imaging technique, the microrobots can be visualized deep into 2 cm, the cell-loaded micro-robot was precisely navigated to desired sites under a gradient magnetic field. Moreover, the carried cells can be spontaneously delivered and the released cells onsite could inhibit the growth of tumors.

To achieve high-resolution tracking and imaging, a microrobot consisting of two layers of hydrogels (thermoresponsive layer of PNIPAM composite hydrogel and a passive layer of PEGDA hydrogel that embedded with radioactive ^{99m}Tc[Tc] for the imaging of single-photon emission computed tomography (SPECT)) were reported (**Figure 6c**) [109]. The magnetic nanoparticles can be used to remotely drive the locomotion of the microrobot, the doped imaging agent of ^{99m}Tc[Tc] allows the microrobot to be monitored in vivo with resolution down to 100 μm in diameter, as well as the detection of shape transformation from tubular to planar configurations resulted from the thermo-responsive PNIPAM hydrogel.

4.3. Biopsy

Benefiting from their small size, biocompatibility, and wireless actuation, small-scale hydrogel-based robots can precisely access hard-to-reach areas and perform minimally invasive or non-invasive biopsy, holding great promise in advanced therapies [110].

Compared to conventional intervention devices for biopsy, small-scale hydrogel-based robots can be implanted in a minimally invasive or non-invasive manner, navigated to target areas, and retrieved the objects to be detected in a minimally invasive or non-invasive way. For instance, a magnetic living hydrogel robot that encapsulates NdFeB particles into polyvinyl alcohol (PVA) hydrogel matrix was utilized for biopsy (**Figure 7a**) [111]. Magnetic living hydrogel robots loaded with genetically engineered bacteria were administered indomethacin (10 mg kg^{-1}) to induce gastrointestinal bleeding in model mice. This robot was actuated by a portable magnet to overcome the barriers of intestinal motility, then the robot was localized and retained by the magnet for a certain period to fulfill the detection. Biochemical detection of fecal pellets showed the effective detection of gastrointestinal bleeding in vivo of the magnetic living hydrogel robot.

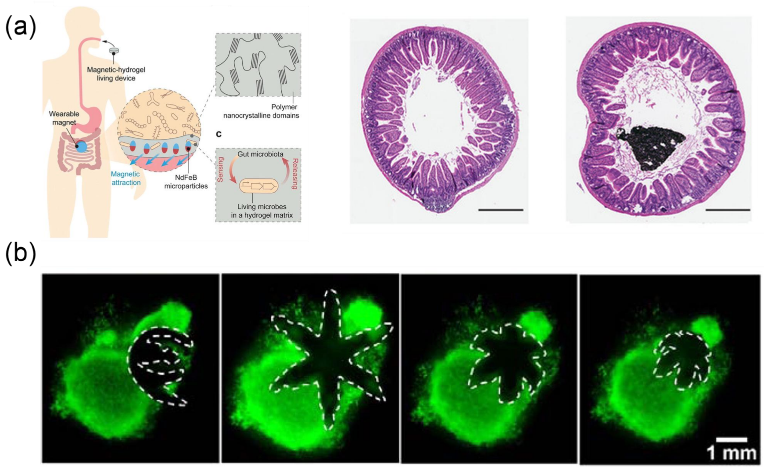

Figure 7. (a) Schematic illustration of a magnetic living hydrogel robot and histological images showing the biopsy. Scale bars: 500 μm. Reproduced with permission from ref. [111]. Copyright John Wiley and Sons., 2021. (b) Capture and excision of cells of a magnetic microgripper. Reproduced with permission from ref. [112]. Copyright American Chemical Society, 2015.

For recycling, small-scale robots that can achieve reversible grasping/releasing and retrieval of target objects would be desirable. For that, a microgripper made of magnetic particles and thermally responsive hydrogels was constructed (**Figure 7b**) [112]. The microgripper entered a miniaturized folded state and was guided to fibroblast cell cluster actuated by an external magnetic field. The microgrippers allowed to open and close to grasp living cells from a fibroblast cell cluster. And the microgripper was easily retrieved controlled by a magnetic field.

4.4. Tissue engineering

Tissue engineering is crucial to repair or create damaged or diseased tissues and organs. Cell- and scaffold-based strategies are effective and popular in tissue engineering [113-115], where emerging small-scale hydrogel-based robots have opened new avenues for cell- and scaffold-based tissue engineering. For example, magnetically actuated double-helical cell microtransporters (76 µm length and 20 µm inner cavity diameter), encoded with mechanical and biological information at the single-cell level, were fabricate by 3D printing [116] (**Figure 8a and 8b**). Under rotating magnetic field, the cell-loaded microbotic helical transporters can move inside confined microchannels following predetermined trajectories. The mesenchymal stem cells maintain osteogenic differentiation capacities when

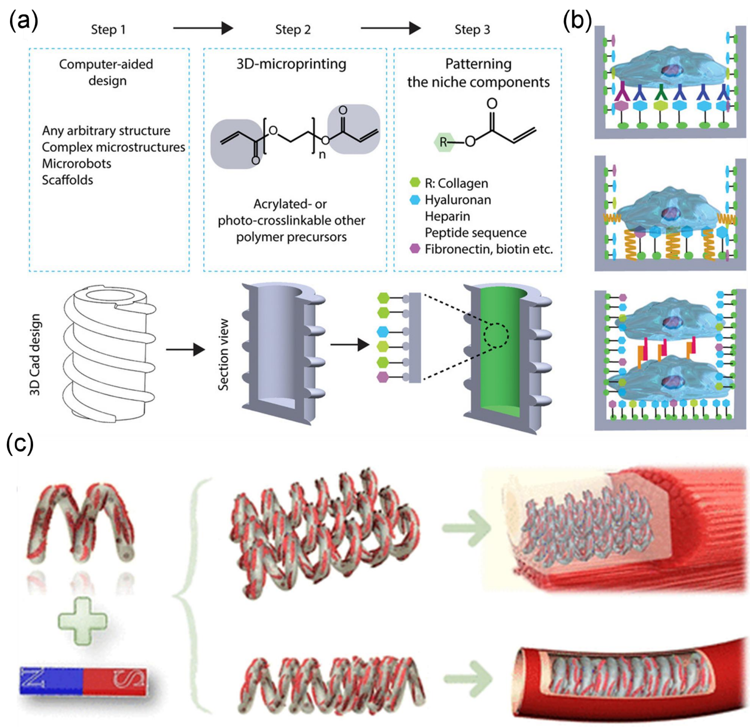

stimulated inside the microswimmers in vitro. Moreover, helical micromotors made of magnetic particles and alginate and GelMA hydrogel were fabricated [117] (**Figure 8c**), they could achieve controllable movements and assemble into different helical geometries under external magnetic field. Upon further incorporating them into biocompatible hydrogel, the helical micromotors form compact stack that provide space for cell growth, which can be used as tissue repairing or blood vessel scaffolds.

Figure 8. (a) Fabrication process of microrobotic transporter. (b) Illustration of interaction between mesenchymal stem cells and microrobotic transporter. Reproduced with permission from ref. [116]. Copyright John Wiley and Sons., 2019. (c) Compact stack or assembly of helical micromotors under the magnetic field for tissue engineering. Reproduced with permission from ref. [117]. Copyright American Chemical Society, 2020.

4.5. Neural stimulation

Neurodegenerative diseases cause traumatic central nervous system injuries and irreversible neural damages [118]. Since small-scale hydrogel-based robots can not only access to targeted regions, but also perform effective therapeutic delivery or wireless neural stimulation, thus holding great potential in such neural diseases. For example, a helical microswimmer consisting of gelatin-methacryloyl (GelMA)-based hydrogel integrated with core-shell magnetoelectric nanoparticles ($CoFe_2O_4$ (CFO) as a core and $BiFeO_3$ (BFO) as a shell) was designed (**Figure 9b and 9b**) [70]. Magnetoelectric nanoparticles not only enabled the magnetic actuation of the

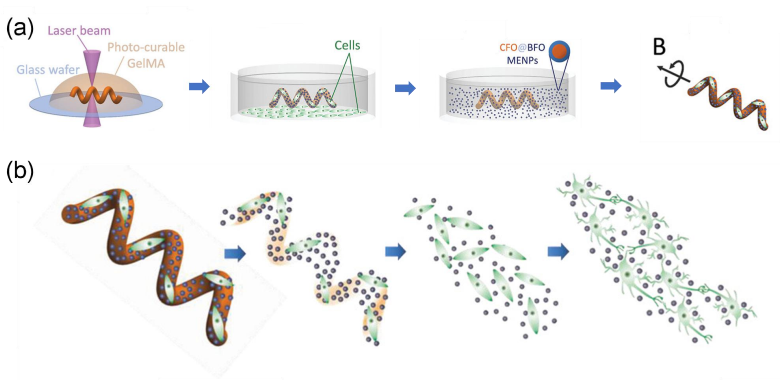

microswimmer, but also generated an electric field under alternating magnetic fields. To be specific, the magnetostrictive CFO core experienced a strain under alternating magnetic fields, which resulted in a transient change in the surface charges of the BFO shell. The change in the transient charge can be used to induce cell differentiation in neuronal cells, which is crucial for the treatment of neurodegenerative diseases.

Figure 9. (b) Fabrication process of helical GelMA microswimmers and (b) Degradation process of the microswimmers and SH-SY5Y cells neuronal differentiation. Reproduced with permission from ref. [70]. copyright John Wiley and Sons., 2020.

5. Summary and outlook

Over the past decade, benefiting from controllable locomotion in different environments due to elastic moduli and mechanical compliance of hydrogels as well as the integration of a variety of complex functions resulting from functionalization and responsiveness of hydrogels, small-scale hydrogel-based robots showing great adaptabilities have largely promoted their biomedical applications including drug and cell delivery, minimally invasive surgery, biopsy, tissue engineering and neural stimulation. Meanwhile, recent attention has been aroused to develop robots that are able to integrate more features such as climbing 3D surfaces and achieving reversible surface adhesion [119], offering possibilities in traversing confined unstructured terrains within human bodies owning to their enhanced adaptabilities. Moreover, to reduce immune inhibition and/or enhance circling life upon entering bodies, hybrid neutrobots were coated with *E. coli* membranes for camouflage. The resulting neutrobots showed similar biological properties to that of natural neutrophils, which greatly enhances the adaptabilities in the human body [120].

Despite great promises of small-scale hydrogel-based robots, they still confront challenges including biomedical safety, large scale fabrication with low cost and high-precision, environmental adaptability, and clinical applications. Great efforts are needed from materials science, chemistry, biology, and engineering for the next-generation small-scale hydrogel-based robots. 1) In terms of safety, although small-scale hydrogel-based robots have been widely used in various biomedical applications, their long-term safety and biocompatibility or biodegradability are still unmet requirements to fulfill the clinical translation. Small-scale hydrogel-based robots fabricated with biocompatible or biodegradable materials (*e.g.* patient blood-derivable biomaterials [121], FDA-approved and natural polymer-based materials) are worth exploring to promote their clinical application in the future. 2) Developing new fabrication facilities or techniques that can achieve large-scale fabrication with low cost and high-precision at the same time is desired. In addition, establishing a database of parameters including material properties, material structures, fabrication methods, locomotion modes and biomedical application scenarios, then one can combine machine learning to achieve tailor-made and intelligent manufacturing. 3) In order to improve their adaptability, on the one hand, improving the manipulation precision of single or swarm small-scale hydrogel-based robot, so that small-scale hydrogel-based robots can complete specific tasks independently or synergistically according to environmental conditions. Establishing a database of motion and environmental parameters to further improve robots' motion accuracy. On the other hand, small-scale hydrogel-based robots are expected to integrate multiple functions such as partition and assembly of robot bodies, camouflage, stealth, *etc* [122, 123]. These multiple functions allow the small-scale hydrogel-based robots better interact with the environment so that they can be finely controlled. 4) A closed-loop system harnessing real-time medical imaging methods to enhance targeted drug delivery/biopsy/surgery is also needed [19, 124]. For future small-scale hydrogel-based robots, we envision that they possess a high level of intelligence like living creatures. Intelligent small-scale hydrogel-based robots can analyze the environmental conditions by themselves with the analysis, perception, and command system, performing various tasks in biomedical applications.

Acknowledgements

The authors acknowledge the financial support provided by National Natural Science Foundation of China (52022102, 52261160380), National Key R&D Program of China (2017YFA0701303), the Youth Innovation Promotion Association of CAS (2019353), Guangdong Regional Joint Fund-Key Project (2021B1515120076), and the Fundamental Research Program of Shenzhen (RCJC20221008092729033, JCYJ20220818101800001).

References

[1] Palagi, S.; Fischer, P. Bioinspired microrobots. *Nat. Rev. Mater.* **2018**, *3*, 113-124.

[2] Hu, W.; Lum, G. Z.; Mastrangeli, M.; Sitti, M. Small-scale soft-bodied robot with multimodal locomotion. *Nature* **2018**, *554*, 81-85.

[3] Nocentini, S.; Parmeggiani, C.; Martella, D.; Wiersma, D. S. Optically driven soft micro robotics. *Adv. Opt. Mater.* **2018**, *6*, 1800207.

[4] Chen, Y.; Yang, J.; Zhang, X.; Feng, Y.; Zeng, H.; Wang, L.; Feng, W. Light-driven bimorph soft actuators: Design, fabrication, and properties. *Mater. Horiz.* **2021**, *8*, 728-757.

[5] Wang, B.; Kostarelos, K.; Nelson, B. J.; Zhang, L. Trends in micro-/nanorobotics: Materials development, actuation, localization, and system integration for biomedical applications. *Adv. Mater.* **2021**, *33*, e2002047.

[6] Park, J.; Kim, J. Y.; Pane, S.; Nelson, B. J.; Choi, H. Acoustically mediated controlled drug release and targeted therapy with degradable 3D porous magnetic microrobots. *Adv. Healthc. Mater.* **2021**, *10*, e2001096.

[7] Chen, X. Z.; Jang, B.; Ahmed, D.; Hu, C.; De Marco, C.; Hoop, M.; Mushtaq, F.; Nelson, B. J.; Pane, S. Small-scale machines driven by external power sources. *Adv. Mater.* **2018**, *30*, e1705061.
[8] Ceylan, H.; Dogan, N. O.; Yasa, I. C.; Musaoglu, M. N.; Kulali, Z. U.; Sitti, M. 3D printed personalized magnetic micromachines from patient blood-derived biomaterials. *Sci. Adv.* **2021**, *7*, eabh0273.
[9] Kim, Y.; Zhao, X. Magnetic soft materials and robots. *Chem. Rev.* **2022**, *122*, 5317-5364.
[10] Koleoso, M.; Feng, X.; Xue, Y.; Li, Q.; Munshi, T.; Chen, X. Micro/nanoscale magnetic robots for biomedical applications. *Mater. Today Bio.* **2020**, *8*, 100085.
[11] Zhang, Y.; Zhang, Y.; Han, Y.; Gong, X. Micro/nanorobots for medical diagnosis and disease treatment. *Micromachines* **2022**, *13, 648*.
[12] Cui, J.; Huang, T. Y.; Luo, Z.; Testa, P.; Gu, H.; Chen, X. Z.; Nelson, B. J.; Heyderman, L. J. Nanomagnetic encoding of shape-morphing micromachines. *Nature* **2019**, *575*, 164-168.
[13] Lee, Y.; Koehler, F.; Dillon, T.; Loke, G.; Kim, Y.; Marion, J.; Antonini, M. J.; Garwood, I. C.; Sahasrabudhe, A.; Nagao, K.; Zhao, X.; Fink, Y.; Roche, E. T.; Anikeeva, P. Magnetically actuated fiber-based soft robots. *Adv. Mater.* **2023**, 10.1002/adma.202301916, e2301916.
[14] Chen, Y.; Chen, D.; Liang, S.; Dai, Y.; Bai, X.; Song, B.; Zhang, D.; Chen, H.; Feng, L. Recent advances in field‐controlled micro‐nano manipulations and micro‐nano robots. *Adv. Intell. Syst.* **2021**, *4*, 2100116.
[15] Cianchetti, M.; Laschi, C.; Menciassi, A.; Dario, P. Biomedical applications of soft robotics. *Nat.Rev. Mater.* **2018**, *3*, 143-153.
[16] Soto, F.; Wang, J.; Ahmed, R.; Demirci, U. Medical micro/nanorobots in precision medicine. *Adv. Sci.* **2020**, *7*, 2002203.
[17] Brown, T. E.; Anseth, K. S. Spatiotemporal hydrogel biomaterials for regenerative medicine. *Chem. Soc. Rev.* **2017**, *46*, 6532-6552.
[18] Wu, Z.; Troll, J.; Jeong, H. H.; Wei, Q.; Stang, M.; Ziemssen, F.; Wang, Z.; Dong, M.; Schnichels, S.; Qiu, T.; Fischer, P. A swarm of slippery micropropellers penetrates the vitreous body of the eye. *Sci. Adv.* **2018**, *4*, eaat4388.
[19] Wu, Z.; Li, L.; Yang, Y.; Hu, P.; Li, Y.; Yang, S. Y.; Wang, L. V.; Gao, W. A microrobotic system guided by photoacoustic computed tomography for targeted navigation in intestines in vivo. *Sci. Robot.* **2019**, *4*, eaax0613.
[20] Chen, M.; Lin, Z.; Xuan, M.; Lin, X.; Yang, M.; Dai, L.; He, Q. Programmable dynamic shapes with a swarm of light-powered colloidal motors. *Angew. Chem. Int. Ed.* **2021**, *60*, 16674-16679.
[21] Liu, X.; Liu, J.; Lin, S.; Zhao, X. Hydrogel machines. *Mater. Today* **2020**, *36*, 102-124.
[22] Apsite, I.; Salehi, S.; Ionov, L. Materials for smart soft actuator systems. *Chem. Rev.* **2022**, *122*, 1349-1415.

[23] Ni, B.; Chen, H.; Zhang, M.; Keller, P.; Tatoulian, M.; Li, M.-H. Thermo-mechanical and photo-luminescence properties of micro-actuators made of liquid crystal elastomers with cyano-oligo (p-phenylene vinylene) crosslinking bridges. *Mater. Chem. Front.* **2019**, *3*, 2499-2506.
[24] Wang, Y.; Cui, H.; Zhao, Q.; Du, X. Chameleon-inspired structural-color actuators. *Matter* **2019**, *1*, 626-638.
[25] Xia, Y.; He, Y.; Zhang, F.; Liu, Y.; Leng, J. A review of shape memory polymers and composites: Mechanisms, materials, and applications. *Adv. Mater.* **2020**, *33*, 2000713.
[26] Hines, L.; Petersen, K.; Lum, G. Z.; Sitti, M. Soft actuators for small-scale robotics. *Adv. Mater.* **2017**, *29*, 1603483.
[27] Zhu, H.; Xu, B.; Wang, Y.; Pan, X.; Qu, Z.; Mei, Y. Self-powered locomotion of a hydrogel water strider. *Sci. Robot.* **2021**, *6*, eabe7925.
[28] Li, C.; Iscen, A.; Palmer, L. C.; Schatz, G. C.; Stupp, S. I. Light-driven expansion of spiropyran hydrogels. *J. Am. Chem. Soc.* **2020**, *142*, 8447-8453.
[29] Banisadr, S.; Chen, J. Infrared actuation-induced simultaneous reconfiguration of surface color and morphology for soft robotics. *Sci. Rep.* **2017**, *7*, 17521.
[30] Choe, A.; Yeom, J.; Kwon, Y.; Lee, Y.; Shin, Y.-E.; Kim, J.; Ko, H. Stimuli-responsive micro/nanoporous hairy skin for adaptive thermal insulation and infrared camouflage. *Mater. Horiz.* **2020**, *7*, 3258-3265.
[31] Erol, O.; Pantula, A.; Liu, W.; Gracias, D. H. Transformer hydrogels: A review. *Adv. Mater. Technol.* **2019**, *4*, 1900043.
[32] Jeon, S. J.; Hauser, A. W.; Hayward, R. C. Shape-morphing materials from stimuli-responsive hydrogel hybrids. *Acc. Chem. Res.* **2017**, *50*, 161-169.
[33] Ding, M.; Jing, L.; Yang, H.; Machnicki, C. E.; Fu, X.; Li, K.; Wong, I. Y.; Chen, P. Y. Multifunctional soft machines based on stimuli-responsive hydrogels: From freestanding hydrogels to smart integrated systems. *Mater. Today Adv.* **2020**, *8*, 100088.
[34] Jiao, D.; Zhu, Q. L.; Li, C. Y.; Zheng, Q.; Wu, Z. L. Programmable morphing hydrogels for soft actuators and robots: From structure designs to active functions. *Acc. Chem. Res.* **2022**, *55*, 1533-1545.
[35] Li, L.; Scheiger, J. M.; Levkin, P. A. Design and applications of photoresponsive hydrogels. *Adv. Mater.* **2019**, *31*, e1807333.
[36] Dong, Y.; Wang, J.; Guo, X.; Yang, S.; Ozen, M. O.; Chen, P.; Liu, X.; Du, W.; Xiao, F.; Demirci, U.; Liu, B. F. Multi-stimuli-responsive programmable biomimetic actuator. *Nat. Commun.* **2019**, *10*, 4087.
[37] Cai, L.; Wang, H.; Yu, Y.; Bian, F.; Wang, Y.; Shi, K.; Ye, F.; Zhao, Y. Stomatocyte structural color-barcode micromotors for multiplex assays. *Natl. Sci. Rev.* **2020**, *7*, 644-651.
[38] Ng, C. S. X.; Tan, M. W. M.; Xu, C.; Yang, Z.; Lee, P. S.; Lum, G. Z. Locomotion of miniature soft robots. *Adv. Mater.* **2021**, *33*, e2003558.
[39] Lin, X.; Xu, B.; Zhu, H.; Liu, J.; Solovev, A.; Mei, Y. Requirement and development of hydrogel micromotors towards biomedical applications. *Research* **2020**, *2020*, 7659749.

[40] Koleoso, M.; Feng, X.; Xue, Y.; Li, Q.; Munshi, T.; Chen, X. Micro/nanoscale magnetic robots for biomedical applications. *Mater. Today Bio.* **2020**, *8*, 100085.

[41] Accardo, J. V.; Kalow, J. A. Reversibly tuning hydrogel stiffness through photocontrolled dynamic covalent crosslinks. *Chem. Sci.* **2018**, *9*, 5987-5993.

[42] Nie, M.; Huang, C.; Du, X. Recent advances in colour-tunable soft actuators. *Nanoscale* **2021**, *13*, 2780-2791.

[43] Bozuyuk, U.; Yasa, O.; Yasa, I. C.; Ceylan, H.; Kizilel, S.; Sitti, M. Light-triggered drug release from 3D-printed magnetic chitosan microswimmers. *ACS Nano* **2018**, *12*, 9617-9625.

[44] Kim, D.; Jo, A.; Imani, K. B. C.; Kim, D.; Chung, J. W.; Yoon, J. Microfluidic fabrication of multistimuli-responsive tubular hydrogels for cellular scaffolds. *Langmuir* **2018**, *34*, 4351-4359.

[45] Hu, N.; Wang, L.; Zhai, W.; Sun, M.; Xie, H.; Wu, Z.; He, Q. Magnetically actuated rolling of star-shaped hydrogel microswimmer. *Macromol. Chem. and Phys.* **2018**, *219*, 1700540.

[46] Hu, X. H.; Yasa, I. C.; Ren, Z. Y.; Goudu, S. R.; Ceylan, H.; Hu, W. Q.; Sitti, M. Magnetic soft micromachines made of linked microactuator networks. *Sci. Adv.* **2021**, *7*, eabe8436.

[47] Kim, D.-i.; Lee, H.; Kwon, S.-h.; Choi, H.; Park, S. Magnetic nano-particles retrievable biodegradable hydrogel microrobot. *Sens. and Actuators B: Chem.* **2019**, *289*, 65-77.

[48] Hu, H.; Nie, M.; Galluzzi, M.; Yu, X.; Du, X. Mimosa-inspired high-sensitive and multi-responsive starch actuators. *Adv. Funct. Mater.*, ***2023***, 2304634.

[49] Wang, X.; Qin, X.-H.; Hu, C.; Terzopoulou, A.; Chen, X.-Z.; Huang, T.-Y.; Maniura-Weber, K.; Pané, S.; Nelson, B. J. 3D printed enzymatically biodegradable soft helical microswimmers. *Adv. Funct. Mater.* **2018**, *28*, 1804107.

[50] Tang, J.; Yao, C.; Gu, Z.; Jung, S.; Luo, D.; Yang, D. Super-soft and super-elastic DNA robot with magnetically driven navigational locomotion for cell delivery in confined space. *Angew. Chem. Int. Ed.* **2020**, *59*, 2490-2495.

[51] Gervasoni, S.; Terzopoulou, A.; Franco, C.; Veciana, A.; Pedrini, N.; Burri, J. T.; de Marco, C.; Siringil, E. C.; Chen, X. Z.; Nelson, B. J.; Puigmarti-Luis, J.; Pane, S. Candybots: A new generation of 3d-printed sugar-based transient small-scale robots. *Adv. Mater.* **2020**, *32*, e2005652.

[52] Li, Z.; Myung, N. V.; Yin, Y. Light-powered soft steam engines for self-adaptive oscillation and biomimetic swimming. *Sci. Robot.* **2021**, *6*, eabi4523.

[53] Xia, N.; Jin, B.; Jin, D.; Yang, Z.; Pan, C.; Wang, Q.; Ji, F.; Iacovacci, V.; Majidi, C.; Ding, Y.; Zhang, L. Decoupling and reprogramming the wiggling motion of midge larvae using a soft robotic platform. *Adv. Mater.* **2022**, *34*, e2109126.

[54] Wu, S.; Hua, M.; Alsaid, Y.; Du, Y.; Ma, Y.; Zhao, Y.; Lo, C. Y.; Wang, C.; Wu, D.; Yao, B.; Strzalka, J.; Zhou, H.; Zhu, X.; He, X. Poly (vinyl alcohol)

hydrogels with broad-range tunable mechanical properties via the hofmeister effect. *Adv. Mater.* **2021**, *33*, e2007829.
[55] Kim, D. I.; Lee, H.; Kwon, S. H.; Sung, Y. J.; Song, W. K.; Park, S. Bilayer hydrogel sheet-type intraocular microrobot for drug delivery and magnetic nanoparticles retrieval. *Adv. Healthc. Mater.* **2020**, *9*, e2000118.
[56] Park, J.; Jin, C.; Lee, S.; Kim, J. Y.; Choi, H. Magnetically actuated degradable microrobots for actively controlled drug release and hyperthermia therapy. *Adv. Healthc. Mater.* **2019**, *8*, e1900213.
[57] Huang, H. W.; Uslu, F. E.; Katsamba, P.; Lauga, E.; Sakar, M. S.; Nelson, B. J. Adaptive locomotion of artificial microswimmers. *Sci. Adv.* **2019**, *5*, eaau1532.
[58] Zhao, X.; Kim, J.; Cezar, C. A.; Huebsch, N.; Lee, K.; Bouhadir, K.; Mooney, D. J. Active scaffolds for on-demand drug and cell delivery. *Proc. Natl. Acad. Sci.* **2011**, *108*, 67-72.
[59] Sun, Z. F.; Yamauchi, Y.; Araoka, F.; Kim, Y. S.; Bergueiro, J.; Ishida, Y.; Ebina, Y.; Sasaki, T.; Hikima, T.; Aida, T. An anisotropic hydrogel actuator enabling earthworm-like directed peristaltic crawling. *Angew. Chem. Int. Ed.* **2018**, *57*, 15772-15776.
[60] Mourran, A.; Zhang, H.; Vinokur, R.; Moller, M. Soft microrobots employing nonequilibrium actuation via plasmonic heating. *Adv. Mater.* **2017**, *29*.
[61] Xin, C.; Jin, D.; Hu, Y.; Yang, L.; Li, R.; Wang, L.; Ren, Z.; Wang, D.; Ji, S.; Hu, K.; Pan, D.; Wu, H.; Zhu, W.; Shen, Z.; Wang, Y.; Li, J.; Zhang, L.; Wu, D.; Chu, J. Environmentally adaptive shape-morphing microrobots for localized cancer cell treatment. *ACS Nano* **2021**, *15*, 18048–18059.
[62] Lee, Y. W.; Chun, S.; Son, D.; Hu, X.; Schneider, M.; Sitti, M. A tissue adhesion-controllable and biocompatible small-scale hydrogel adhesive robot. *Adv. Mater.* **2022**, *34*, e2109325.
[63] Hu, H.; Huang, C.; Galluzzi, M.; Ye, Q.; Xiao, R.; Yu, X.; Du, X. Editing the shape morphing of monocomponent natural polysaccharide hydrogel films. *Research* **2021**, *2021*, 9786128.
[64] Du, X.; Cui, H.; Zhao, Q.; Wang, J.; Chen, H.; Wang, Y. Inside-out 3D reversible ion-triggered shape-morphing hydrogels. *Research* **2019**, *2019*, 6398296.
[65] Wang, S.; Zhao, Q.; Li, J.; Du, X. Morphing-to-adhesion polysaccharide hydrogel for adaptive biointerfaces. *ACS Appl. Mater. Interfaces* **2022**, *14*, 42420–42429.
[66] Zhang, S.; Ke, X.; Jiang, Q.; Chai, Z.; Wu, Z.; Ding, H. Fabrication and functionality integration technologies for small-scale soft robots. *Adv. Mater.* **2022**, *34*, e2200671.
[67] Tasoglu, S.; Diller, E.; Guven, S.; Sitti, M.; Demirci, U. Untethered micro-robotic coding of three-dimensional material composition. *Nat. Commun.* **2014**, *5*, 3124.
[68] Xie, M.; Zhang, W.; Fan, C.; Wu, C.; Feng, Q.; Wu, J.; Li, Y.; Gao, R.; Li, Z.; Wang, Q.; Cheng, Y.; He, B. Bioinspired soft microrobots with precise

magneto-collective control for microvascular thrombolysis. *Adv. Mater.* **2020**, *32*, e2000366.
[69] Wu, Z.; Lin, X.; Zou, X.; Sun, J.; He, Q. Biodegradable protein-based rockets for drug transportation and light-triggered release. *ACS Appl. Mater. Interfaces* **2015**, *7*, 250-255.
[70] Dong, M.; Wang, X.; Chen, X. Z.; Mushtaq, F.; Deng, S.; Zhu, C.; Torlakcik, H.; Terzopoulou, A.; Qin, X. H.; Xiao, X.; Puigmartí‐Luis, J.; Choi, H.; Pêgo, A. P.; Shen, Q. D.; Nelson, B. J.; Pané, S. 3D-printed soft magnetoelectric microswimmers for delivery and differentiation of neuron-like cells. *Adv. Funct. Mater.* **2020**, *30*, 1910323.
[71] Wallin, T. J.; Pikul, J.; Shepherd, R. F. 3D printing of soft robotic systems. *Nat. Rev. Mater.* **2018**, *3*, 84-100.
[72] Peters, C.; Hoop, M.; Pane, S.; Nelson, B. J.; Hierold, C. Degradable magnetic composites for minimally invasive interventions: Device fabrication, targeted drug delivery, and cytotoxicity tests. *Adv. Mater.* **2016**, *28*, 533-538.
[73] Llacer-Wintle, J.; Rivas-Dapena, A.; Chen, X. Z.; Pellicer, E.; Nelson, B. J.; Puigmarti-Luis, J.; Pane, S. Biodegradable small-scale swimmers for biomedical applications. *Adv. Mater.* **2021**, *33*, e2102049.
[74] Adam, G.; Benouhiba, A.; Rabenorosoa, K.; Clévy, C.; Cappelleri, D. J. 4d printing: Enabling technology for microrobotics applications. *Adv. Intell. Syst.***2021**, *3*, 2000216.
[75] Champeau, M.; Heinze, D. A.; Viana, T. N.; de Souza, E. R.; Chinellato, A. C.; Titotto, S. 4D printing of hydrogels: A review. *Adv. Funct. Mater.* **2020**, *30*, 1910606.
[76] Gao, C.; Wang, Y.; Ye, Z.; Lin, Z.; Ma, X.; He, Q. Biomedical micro-/nanomotors: From overcoming biological barriers to in vivo imaging. *Adv. Mater.* **2021**, *33*, e2000512.
[77] Dong, Y.; Wang, L.; Iacovacci, V.; Wang, X.; Zhang, L.; Nelson, B. J. Magnetic helical micro-/nanomachines: Recent progress and perspective. *Matter* **2022**, *5*, 77-109.
[78] Zhou, H.; Mayorga-Martinez, C. C.; Pane, S.; Zhang, L.; Pumera, M. Magnetically driven micro and nanorobots. *Chem. Rev.* **2021**, *121*, 4999-5041.
[79] Lahikainen, M.; Zeng, H.; Priimagi, A. Reconfigurable photoactuator through synergistic use of photochemical and photothermal effects. *Nat. Commun.* **2018**, *9*, 4148.
[80] Tu, Y.; Peng, F.; Sui, X.; Men, Y.; White, P. B.; van Hest, J. C. M.; Wilson, D. A. Self-propelled supramolecular nanomotors with temperature-responsive speed regulation. *Nat. Chem.* **2017**, *9*, 480-486.
[81] Mou, F.; Chen, C.; Zhong, Q.; Yin, Y.; Ma, H.; Guan, J. Autonomous motion and temperature-controlled drug delivery of Mg/Pt-poly (n-isopropylacrylamide) janus micromotors driven by simulated body fluid and blood plasma. *ACS Appl. Mater. Interfaces* **2014**, *6*, 9897-9903.
[82] Li, M.; Zhang, H.; Liu, M.; Dong, B. Motion-based glucose sensing based on a fish-like enzymeless motor. *J. Mater. Chem. C* **2017**, *5*, 4400-4407.

[83] Soto, F.; Martin, A.; Ibsen, S.; Vaidyanathan, M.; Garcia-Gradilla, V.; Levin, Y.; Escarpa, A.; Esener, S. C.; Wang, J. Acoustic microcannons: Toward advanced microballistics. *ACS Nano* **2016**, *10*, 1522-1528.
[84] Gelebart, A. H.; Jan Mulder, D.; Varga, M.; Konya, A.; Vantomme, G.; Meijer, E. W.; Selinger, R. L. B.; Broer, D. J. Making waves in a photoactive polymer film. *Nature* **2017**, *546*, 632-636.
[85] Gan, T.; Shang, W.; Handschuh-Wang, S.; Zhou, X. Light-induced shape morphing of liquid metal nanodroplets enabled by polydopamine coating. *Small* **2019**, *15*, e1804838.
[86] Sun, B.; Jia, R.; Yang, H.; Chen, X.; Tan, K.; Deng, Q.; Tang, J. Magnetic arthropod millirobots fabricated by 3D-printed hydrogels. *Adv. Intell. Syst.***2021**, *4*, 2100139.
[87] Kim, Y.; Parada, G. A.; Liu, S.; Zhao, X. Ferromagnetic soft continuum robots. *Sci. Robot.* **2019**, *4*, eaax7329.
[88] Li, Z.; Li, Y.; Chen, C.; Cheng, Y. Magnetic-responsive hydrogels: From strategic design to biomedical applications. *J. Control. Release* **2021**, *335*, 541-556.
[89] Liang, S.; Tu, Y.; Chen, Q.; Jia, W.; Wang, W.; Zhang, L. Microscopic hollow hydrogel springs, necklaces and ladders: A tubular robot as a potential vascular scavenger. *Mater. Horiz.* **2019**, *6*, 2135-2142.
[90] Liu, X.; Kent, N.; Ceballos, A.; Streubel, R.; Jiang, Y.; Chai, Y.; Kim, P. Y.; Forth, J.; Hellman, F.; Shi, S.; Wang, D.; Helms, B. A.; Ashby, P. D.; Fischer, P.; Russell, T. P. Reconfigurable ferromagnetic liquid droplets. *Science* **2019**, *365*, 264-267.
[91] Sun, L.; Chen, Z.; Bian, F.; Zhao, Y. Bioinspired soft robotic caterpillar with cardiomyocyte drivers. *Adv. Funct. Mater.* **2019**, *30*, 1907820.
[92] Sun, L.; Yu, Y.; Chen, Z.; Bian, F.; Ye, F.; Sun, L.; Zhao, Y. Biohybrid robotics with living cell actuation. *Chem. Soc. Rev.* **2020**, *49*, 4043-4069.
[93] Cvetkovic, C.; Raman, R.; Chan, V.; Williams, B. J.; Tolish, M.; Bajaj, P.; Sakar, M. S.; Asada, H. H.; Saif, M. T.; Bashir, R. Three-dimensionally printed biological machines powered by skeletal muscle. *Proc. Natl. Acad. Sci.* **2014**, *111*, 10125-10130.
[94] Li, M.; Wang, X.; Dong, B.; Sitti, M. In-air fast response and high speed jumping and rolling of a light-driven hydrogel actuator. *Nat. Commun.* **2020**, *11*, 3988.
[95] Zheng, Z.; Wang, H.; Dong, L.; Shi, Q.; Li, J.; Sun, T.; Huang, Q.; Fukuda, T. Ionic shape-morphing microrobotic end-effectors for environmentally adaptive targeting, releasing, and sampling. *Nat. Commun.* **2021**, *12*, 411.
[96] Huang, H. W.; Sakar, M. S.; Petruska, A. J.; Pane, S.; Nelson, B. J. Soft micromachines with programmable motility and morphology. *Nat. Commun.* **2016**, *7*, 12263.
[97] Du, X.; Cui, H.; Xu, T.; Huang, C.; Wang, Y.; Zhao, Q.; Xu, Y.; Wu, X. Reconfiguration, camouflage, and color ‐ shifting for bioinspired adaptive hydrogel-based millirobots. *Adv. Funct. Mater.* **2020**, *30*, 1909202.

[98] Shah, D.; Yang, B.; Kriegman, S.; Levin, M.; Bongard, J.; Kramer-Bottiglio, R. Shape changing robots: Bioinspiration, simulation, and physical realization. *Adv. Mater.* **2021**, *33*, e2002882.
[99] Medina-Sánchez, M.; Magdanz, V.; Guix, M.; Fomin, V. M.; Schmidt, O. G. Swimming microrobots: Soft, reconfigurable, and smart. *Adv. Funct. Mater.* **2018**, *28*, 1707228.
[100] Sun, M.; Tian, C.; Mao, L.; Meng, X.; Shen, X.; Hao, B.; Wang, X.; Xie, H.; Zhang, L. Reconfigurable magnetic slime robot: Deformation, adaptability, and multifunction. *Adv. Funct. Mater.* **2022**, *32*, 2112508.
[101] Manzari, M. T.; Shamay, Y.; Kiguchi, H.; Rosen, N.; Scaltriti, M.; Heller, D. A. Targeted drug delivery strategies for precision medicines. *Nat. Rev. Mater.* **2021**, *6*, 351-370.
[102] Cai, L.; Zhao, C.; Chen, H.; Fan, L.; Zhao, Y.; Qian, X.; Chai, R. Suction-cup-inspired adhesive micromotors for drug delivery. *Adv. Sci.* **2022**, *9*, e2103384.
[103] Chen, H.; Zhang, H.; Xu, T.; Yu, J. An overview of micronanoswarms for biomedical applications. *ACS Nano* **2021**, *15*, 15625-15644.
[104] Ceylan, H.; Yasa, I. C.; Yasa, O.; Tabak, A. F.; Giltinan, J.; Sitti, M. 3d-printed biodegradable microswimmer for theranostic cargo delivery and release. *ACS Nano* **2019**, *13*, 3353-3362.
[105] Zhang, X.; Chen, G.; Fu, X.; Wang, Y.; Zhao, Y. Magneto-responsive microneedle robots for intestinal macromolecule delivery. *Adv. Mater.* **2021**, *33*, e2104932.
[106] Li, H.; Go, G.; Ko, S. Y.; Park, J.-O.; Park, S. Magnetic actuated pH-responsive hydrogel-based soft micro-robot for targeted drug delivery. *Smart Mater. Struct.* **2016**, *25*, 027001.
[107] Fusco, S.; Sakar, M. S.; Kennedy, S.; Peters, C.; Bottani, R.; Starsich, F.; Mao, A.; Sotiriou, G. A.; Pane, S.; Pratsinis, S. E.; Mooney, D.; Nelson, B. J. An integrated microrobotic platform for on-demand, targeted therapeutic interventions. *Adv. Mater.* **2014**, *26*, 952-957.
[108] Wei, T.; Liu, J.; Li, D.; Chen, S.; Zhang, Y.; Li, J.; Fan, L.; Guan, Z.; Lo, C. M.; Wang, L.; Man, K.; Sun, D. Development of magnet-driven and image-guided degradable microrobots for the precise delivery of engineered stem cells for cancer therapy. *Small* **2020**, *16*, e1906908.
[109] Iacovacci, V.; Blanc, A.; Huang, H.; Ricotti, L.; Schibli, R.; Menciassi, A.; Behe, M.; Pané, S.; Nelson, B. J. High-resolution spect imaging of stimuli-responsive soft microrobots. *Small* **2019**, *15*, 1900709.
[110] Zhu, J.; Lyu, L.; Xu, Y.; Liang, H.; Zhang, X.; Ding, H.; Wu, Z. Intelligent soft surgical robots for next-generation minimally invasive surgery. *Adv. Intell. Syst.* **2021**, *3*, 2100011.
[111] Liu, X.; Yang, Y.; Inda, M. E.; Lin, S.; Wu, J.; Kim, Y.; Chen, X.; Ma, D.; Lu, T. K.; Zhao, X. Magnetic living hydrogels for intestinal localization, retention, and diagnosis. *Adv. Funct. Mater.* **2021**, *31*, 2010918.

[112] Breger, J. C.; Yoon, C.; Xiao, R.; Kwag, H. R.; Wang, M. O.; Fisher, J. P.; Nguyen, T. D.; Gracias, D. H. Self-folding thermo-magnetically responsive soft microgrippers. *ACS Appl. Mater. Interfaces* **2015**, *7*, 3398-3405.
[113] Cai, L.; Xu, D.; Chen, H.; Wang, L.; Zhao, Y. Designing bioactive micro-/nanomotors for engineered regeneration. *Engineered Regeneration* **2021**, *2*, 109-115.
[114] Peng, M.; Zhao, Q.; Wang, M.; Du, X. Reconfigurable scaffolds for adaptive tissue regeneration. *Nanoscale* **2023**, *15*, 6105-6120.
[115] Zhao, Q.; Wang, J.; Cui, H.; Chen, H.; Wang, Y.; Du, X. Programmed shape-morphing scaffolds enabling facile 3D endothelialization. *Adv. Funct. Mater.* **2018**, *28*, 1801027.
[116] Yasa, I. C.; Tabak, A. F.; Yasa, O.; Ceylan, H.; Sitti, M. 3D-printed microrobotic transporters with recapitulated stem cell niche for programmable and active cell delivery. *Adv. Funct. Mater.* **2019**, *29*, 1808992.
[117] Yu, Y.; Guo, J.; Wang, Y.; Shao, C.; Wang, Y.; Zhao, Y. Bioinspired helical micromotors as dynamic cell microcarriers. *ACS Appl. Mater. Interfaces* **2020**, *12*, 16097-16103.
[118] Lee, H. G.; Wheeler, M. A.; Quintana, F. J. Function and therapeutic value of astrocytes in neurological diseases. *Nat. Rev. Drug Discov.* **2022**, *21*, 339-358.
[119] Liu, K.; Hacker, F.; Daraio, C. Robotic surfaces with reversible, spatiotemporal control for shape morphing and object manipulation. *Sci. Robot.* **2021**, *6*.
[120] Zhang, H.; Li, Z.; Gao, C.; Fan, X.; Pang, Y.; Li, T.; Wu, Z.; Xie, H.; He, Q. Dual-responsive biohybrid neutrobots for active target delivery. *Sci. Robot.* **2021**, *6*, eaaz9519.
[121] Zhu, Z.; Park, H. S.; McAlpine, M. C. 3D printed deformable sensors. *Sci. Adv.* **2020**, *6*, eaba5575.
[122] Wang, F.; Liu, M.; Liu, C.; Zhao, Q.; Wang, T.; Wang, Z.; Du, X. Light-induced charged slippery surfaces. *Sci. Adv.* **2022**, *8*, eabp9369.
[123] Wang, F.; Liu, M.; Liu, C.; Huang, C.; Zhang, L.; Cui, A.; Hu, Z.; Du, X. Light control of droplets on photo-induced charged surfaces. *Natl. Sci. Rev.* **2022**, *10,* nwac164.
[124] Yan, X.; Zhou, Q.; Vincent, M.; Deng, Y.; Yu, J.; Xu, J.; Xu, T.; Tang, T.; Bian, L.; Wang, Y. J.; Kostarelos, K.; Zhang, L. Multifunctional biohybrid magnetite microrobots for imaging-guided therapy. *Sci. Robot.* **2017**, *2*, eaaq1155.